INSTITUTE OF PHYSICS PUBLISHING JOURNAL OF PHYSICS: CONDENSED MATTER

J. Phys.: Condens. Matter **16** (2004) S4103–S4114 PII: S0953-8984(04)78940-7

Colloids in inhomogeneous external magnetic fields: particle tweezing, trapping and void formation

V A Froltsov, C N Likos and H Löwen

Institut für Theoretische Physik II, Heinrich-Heine-Universität Düsseldorf, Universitätsstraße 1, D-40225 Düsseldorf, Germany

Received 5 April 2004
Published 10 September 2004
Online at stacks.iop.org/JPhysCM/16/S4103
doi:10.1088/0953-8984/16/38/025

Abstract

Two-dimensional super-paramagnetic suspensions that are confined to a planar liquid–gas interface and exposed to an inhomogeneous external magnetic field directed perpendicular to the interface are studied by extensive Monte Carlo computer simulations. The external field is a superposition of a homogeneous field and a localized inhomogeneity, modelled by a Gaussian function. The inhomogeneity causes two combined effects that compete against each other: it provides an external potential, modifying at the same time the mutual interparticle repulsion. If the inhomogeneity enhances the strength of the homogeneous profile, the inhomogeneous field is a 'magnetic tweezer' for low particle densities. At higher densities, on the other hand, there is a small accumulation in the centre of the inhomogeneous field, which leads to a depletion zone outside the inhomogeneity due to the mutual interparticle repulsion. Very large inhomogeneities produce local crystallites surrounded by a depletion ring. If the inhomogeneity reduces the total field strength, particles are repelled from the inhomogeneity and voids are generated in the suspension. Our predictions are of relevance to the direct transport of magnetic particles and can be verified in real-space experiments of super-paramagnetic suspensions.

1. Introduction

Trapping particles in a controlled way by external electromagnetic fields is the key to studying properties of strongly confined few-particle systems. For example, Bose–Einstein condensation was observed in a system of a few atomic ions confined by a quadrupolar trap [1]. Trapping is also very important for colloidal particles as used, for example, by the optical-tweezer method [2]. Here a laser-optical field is used to grasp single particles, since their dielectric contrast to the solvent makes it energetically more favourable to stay inside the focused laser beams where the intensity is maximal [3]. The optical-tweezing method has been used to study the effective interactions between particles [4], to investigate hydrodynamic interactions [5, 6], to pattern surfaces by adsorbed colloids [7], and to perform controlled

pulling experiment of DNA chains that are attached on a polystyrene sphere [8]. While optical tweezers typically grasp a single colloidal particle, larger traps, like the so-called 'dielectric bottle', have been used to attract a large number of particles optically [9]: a high electric field between capacitor plates is used to pull colloidal particles out of the solution. This effect allows controlling of the assembly of colloidal particles by an external drive (i.e., the external field), a possibility that bears significant relevance, for example, in the construction of microfluidic devices [10].

In this paper, we report on the two-dimensional *magnetic* analogue of the optical tweezer and the dielectric bottle. We study here super-paramagnetic colloidal particles that are confined by gravity to the two-dimensional air–water interface of a pendant drop [11–14]. Typically, these particles are subjected to a constant external magnetic field which is directed perpendicular to the air–water interface. The external field then induces a strong magnetic moment in each of the colloidal particles, which leads to a mutual repulsion between aligned dipoles. Preceding studies have considered homogeneous fields and also magnetic suspensions in a gravitational field that does not affect the interparticle interactions [15, 16]. In this work, we focus on non-homogeneous external magnetic fields which are, for simplicity, always directed perpendicular to the air–water interface.

In detail, we consider a superposition of a basic homogeneous field and a localized 'trapping field'. This situation is realized experimentally by superimposing two small coils on top of each other to the experimental sample (see figure 1). The inhomogeneity causes two combined and competing effects: it provides an external potential but it also modifies the mutual interparticle repulsion. We use extensive Monte Carlo computer simulation studies to calculate the one-particle equilibrium density profiles of the magnetic colloids in the inhomogeneous field. We find a wealth of different behaviour including a magnetic tweezer, a magnetic trap which generates small crystallites of the size of the field-inhomogeneity, and void generation. The behaviour depends crucially on the sign of the magnetic trapping field relative to the homogeneous field, and on the concentration of the colloids. If the inhomogeneous field points parallel to the homogeneous one, the inhomogeneous field acts as a 'magnetic tweezer' at small particle densities. At higher densities, on the other hand, there is a small accumulation in the centre of the inhomogeneous field which leads to a depletion zone outside the inhomogeneities due to the mutual interparticle repulsion. Very large inhomogeneities produce local crystallites surrounded by a depletion ring. If the inhomogeneity points antiparallel to the homogeneous field, on the other hand, particles are repelled from the inhomogeneity, and voids are generated in the suspension.

The rest of the paper is organized as follows. In section 2, we define the model Hamiltonian used, which was derived previously in [17]. The simulation method and results for the density fields for different inhomogeneities are presented in section 3. We finally conclude in section 4.

2. The model

We consider a two-dimensional system of super-paramagnetic colloidal particles interacting with each other via the dipole–dipole pair potential, valid for point-like magnetic dipoles,

$$u^{\mathrm{dd}}(\mathbf{r}, \mathbf{m}_i, \mathbf{m}_j) = \frac{1}{2}\frac{\mathbf{m}_i \cdot \mathbf{m}_j - 3(\mathbf{m}_i \cdot \mathbf{n})(\mathbf{m}_j \cdot \mathbf{n})}{r^3}, \tag{1}$$

where $\mathbf{r} = \mathbf{r}_i - \mathbf{r}_j$ is the interparticle separation vector, $\mathbf{n} = \mathbf{r}/r$ is the unit vector along the line connecting the centres of the colloids, and $\mathbf{m}_i$ and $\mathbf{m}_j$ are the magnetic moments carried by particles i and j ($i \neq j$). The factor $1/2$ in equation (1) appears due to the paramagnetic nature of colloids, i.e., it stems from the fact that the dipoles on the particles are not permanent but

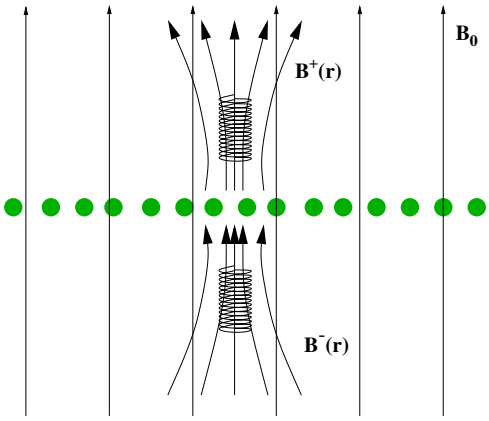

Figure 1. A sketch of an experimental set-up that could be used in order to generate locally inhomogeneous magnetic fields that are perpendicular to the interface in which the paramagnetic particles are located. The thin vertical lines denote the homogeneous field $\mathbf{B}_0$, whereas the thick ones denote field lines generated by the upper and lower coils, $\mathbf{B}^+(\mathbf{r})$ and $\mathbf{B}^-(\mathbf{r})$, respectively. The paramagnetic particles are denoted as filled spheres in the middle of the picture.

(This figure is in colour only in the electronic version)

rather induced by the external magnetic field. A detailed derivation of the interaction energy u of two polarizable particles i and j in an arbitrarily varying external field is presented in [17] and reads as follows:

$$u = u^{\mathrm{dd}}(\mathbf{r}, \mathbf{m}_i, \mathbf{m}_j) - \tfrac{1}{2}\mathbf{m}_i \cdot \mathbf{B}_0(\mathbf{r}_i) - \tfrac{1}{2}\mathbf{m}_j \cdot \mathbf{B}_0(\mathbf{r}_j). \tag{2}$$

Here u^{dd} is defined in equation (1), and the last two terms describe the particle interaction with the field. If the external field is homogeneous, the latter turn into an irrelevant constant whose effect can be absorbed into a rescaling of the chemical potential μ of the particles. However, in case of *inhomogeneous* magnetic field, which we consider in this paper, the particle–field interaction term cannot be ignored any more and it has prominent physical consequences, as we demonstrate in what follows. Finally, we remark that the overall field energy term has been subtracted in equation (2).

In our problem the colloids are spherical with a finite extent, but, for the sake of simplicity, we consider their magnetic dipoles as point-like. Their motion is confined on the plane formed by the water–air interface. This two-dimensional system consisting of N particles is placed under a spatially inhomogeneous magnetic field $\mathbf{B}_0(\mathbf{r})$ directed perpendicular to the interface, which induces in each particle a magnetic moment $\mathbf{m}_i$, $i = 1, 2, \ldots, N$. In this paper we consider super-paramagnetic colloids [13] for which the magnetic moment $\mathbf{m}_i$ completely aligns with the external field $\mathbf{B}_0$ and the following relation holds:

$$\mathbf{m}_i = \chi \mathbf{B}_0, \tag{3}$$

where χ is the magnetic susceptibility of the particles, which, for super-paramagnetic particles, has a value typically lying in the range $1\ \mu\mathrm{m}^3 \lesssim \chi \lesssim 10\ \mu\mathrm{m}^3$ [12][1].

Assuming pair additivity of the interactions, the total Hamiltonian $\mathcal{H}$ of the two-dimensional system of super-paramagnetic colloids under a perpendicular magnetic field takes the form

$$\mathcal{H} = \sum_i \frac{p_i^2}{2m} + \sum_{i<j} \frac{\chi^2}{2} \frac{B_0(\mathbf{r}_i) B_0(\mathbf{r}_j)}{|\mathbf{r}_i - \mathbf{r}_j|^3} - \sum_i \frac{\chi}{2} B_0^2(\mathbf{r}_i), \tag{4}$$

[1] Note that we are using Gaussian units throughout, in which χ has the dimensions of volume.

where the first term is the total kinetic energy, with the momenta $\mathbf{p}_i$ and the mass m of the particles, the second term is the dipole–dipole interaction, and the last term accounts for the particle–field interaction. The configuration of the system is determined in general by the competition between repulsive dipole–dipole interaction and attractive dipole–field interaction. To model the field inhomogeneity we use a Gaussian superimposed to the homogeneous magnetic field of B_0-strength such that the total field is

$$B_0(\mathbf{r}) = B_0[1 + a_0 \mathrm{e}^{-(r/l)^2}]. \tag{5}$$

Here a_0 and l are the height and the width of the Gaussian, respectively.

A physical realization of a *local* and *perpendicular* magnetic field can be experimentally achieved by applying a set-up such as the one shown in figure 1. One can imagine positioning two identical coils of the same helicity symmetrically on either side of the confining interface. On sending electrical currents into both coils, one generates two magnetic fields, $\mathbf{B}^+(\mathbf{r})$ from the upper coil and $\mathbf{B}^-(\mathbf{r})$ from the lower one. If the currents are equal in strength and flow in the same direction on both coils, then the components of the fields $\mathbf{B}^+(\mathbf{r})$ and $\mathbf{B}^-(\mathbf{r})$ that are tangential to the interface cancel each other and only an additional *perpendicular* component remains. Depending on the direction of the current on the coils, this remaining component can be either parallel to the wide external field $\mathbf{B}_0$, causing thereby a local enhancement of the magnetic field strength, or antiparallel to it, causing a local weakening of the latter. We also note that if one sends the currents into the coils in *opposite* directions, then an additional local field that it purely *tangential* to the confining interface is obtained. In any case, the total magnetic field acting on the particles reads as

$$\mathbf{B}_0(\mathbf{r}) = \mathbf{B}_0 + \mathbf{B}^+(\mathbf{r}) + \mathbf{B}^-(\mathbf{r}). \tag{6}$$

The relative strength of the dipolar interaction is characterized by the dimensionless coupling constant

$$\Gamma = \frac{(\chi B_0)^2}{k_\mathrm{B} T}(\pi\rho_0)^{3/2}, \tag{7}$$

where k_B denotes Boltzmann's constant, T the absolute temperature, and ρ_0 is the density of the homogeneous system, i.e., the value of the density far away from the localized magnetic field inhomogeneity. We further define the average interparticle distance a as $a = \rho_0^{-1/2}$. Changing the parameter Γ allows tuning of the repulsion between the particles, ranging from weakly ($\Gamma \ll 1$) to strongly ($\Gamma \gg 1$) interacting systems. Thus, a local enhancement of the field results in a strengthening of the interparticle repulsions. On the other hand, the third term on the right-hand side of equation (4) causes the particles to be attracted to a magnetic 'trap', in which the total field is locally stronger than its homogeneous value B_0 at $r \to \infty$. Two terms with competing effects are thus present in the Hamiltonian, and the net resulting density profiles depend on concentration of the colloids, as well as on the sign of the Gaussian bulge, i.e., on the sign of a_0.

3. Results and discussion

In order to study the effect of an inhomogeneous magnetic field in the form of equation (5) on the behaviour of the colloids, we have performed extensive Monte Carlo simulations in the grand-canonical (μ, V, T) ensemble[2]. The standard grand-canonical sampling technique was used (see for example [18]), with typical runs consisting of 25×10^6–50×10^6 steps with 50×10^3 steps used for equilibration. The typical size of the simulation box ranged between

[2] In our two-dimensional system, the volume V has the meaning of the area A.

$20a$ and $40a$, with the average interparticle distance a (or $10l$ and $20l$, with the trap width l). We have calculated the equilibrium one-particle density profiles $\rho(r)$ as averages during the simulation, as well as the coverage parameter C defined as

$$C = 2\pi \int_0^\infty r[\rho(r) - \rho_0]\,\mathrm{d}r. \tag{8}$$

The coverage C is a reasonable measure of the *enhancing* or *depleting* effects of the local potential, as it expresses the excess number of particles that are drawn into ($C > 0$) or pushed away ($C < 0$) from the system in the presence of the Gaussian bulge.

In what follows, the average interparticle distance a of the uniform system is used as the length scale. Introducing the dimensionless variables $\mathbf{x} = \mathbf{r}/a$ and $\bar{l} = l/a$, we can recast the Hamiltonian of the system, equation (4), in the form

$$\beta\mathcal{H} = \sum_i \frac{\beta \mathbf{p}_i^2}{2m} + \sum_{i<j} \frac{\Gamma}{2\pi^{3/2}|\mathbf{x}_i - \mathbf{x}_j|^3}[1 + a_0 \mathrm{e}^{-(x_i/\bar{l})^2}][1 + a_0 \mathrm{e}^{-(x_j/\bar{l})^2}]$$
$$- \sum_i \frac{\Gamma}{2\pi^{3/2}} \left(\frac{a^3}{\chi}\right)[1 + a_0 \mathrm{e}^{-(x_i/\bar{l})^2}]^2, \tag{9}$$

where $\beta = (k_\mathrm{B}T)^{-1}$. Note that there are four parameters characterizing the system: Γ, a_0, $\bar{l}$ and χ, whereas only one, Γ, remains for the homogeneous case, $a_0 = 0$. The dimensionless ratio $\lambda = a^3/\chi$ in equation (9) is somewhat special because its value cannot be varied arbitrarily if we change Γ. Assuming that we keep $\mathbf{B}_0$ and the temperature fixed and we control Γ through the chemical potential μ, then since $\Gamma \propto a^{-3}$, it follows that the parameters $\lambda_{1,2}$ corresponding to two different values $\Gamma_{1,2}$ are *physically* related to each other through

$$\lambda_2 = \lambda_1 \frac{\Gamma_1}{\Gamma_2}. \tag{10}$$

We have thus fixed in our simulations the value of λ for one particular choice of Γ: $\lambda = 15.1$ for $\Gamma = 7.4$, a realistic value if we take $\chi \cong 8\ \mu\mathrm{m}^3$ and a typical interparticle distance $a \cong 5\ \mu\mathrm{m}$. Since we simulated in the grand canonical ensemble, in all subsequent simulations at different Γ-values equation (10) was satisfied automatically. By varying the parameters a_0, $\bar{l}$ and Γ we have investigated the effects of the strength and range of the inhomogeneity as well as those of coupling in the resulting profiles.

First we consider very low densities, in which case the particles can be approximated as being noninteracting and the second term on the right-hand side of equation (4) can be ignored. The inhomogeneous density profile $\rho(\mathbf{r})$ is then trivially obtained as

$$\rho(\mathbf{r}) = \mathrm{e}^{\mu/k_\mathrm{B}T} \mathrm{e}^{\chi B_0^2(\mathbf{r})/(2k_\mathrm{B}T)}/\Lambda^2, \tag{11}$$

with the thermal de Broglie wavelength $\Lambda = \sqrt{2\pi\hbar^2/(mk_\mathrm{B}T)}$ and Planck's constant $\hbar$. In this case, the particles are simply attracted to the trap ($a_0 > 0$), and since the total magnetic field strength $B_0(\mathbf{r})$ appears in the exponent of equation (11), the coverage is clearly positive. For strong trapping at low densities, a single particle is caught by the inhomogeneity, which results in the magnetic tweezer effect. Under the assumption of weak trapping, $a_0 \ll 1$, on the other hand, an analytic expression for the coverage can be obtained that reads as

$$C \cong \frac{\Gamma}{2\sqrt{\pi}} a_0 \lambda \bar{l}^2 = \frac{\chi B_0^2}{2k_\mathrm{B}T} \pi a_0 \bar{l}^2. \tag{12}$$

Hence, in the case of weak interactions, the coverage resulting from a trap scales linearly with the trap's strength a_0 and quadratically with its width $\bar{l}$.

Next we consider the case of moderate couplings and we set $\Gamma = 7.4$, a coupling for which the system is fluid in the homogeneous case; indeed, the bulk freezing transition of a system of

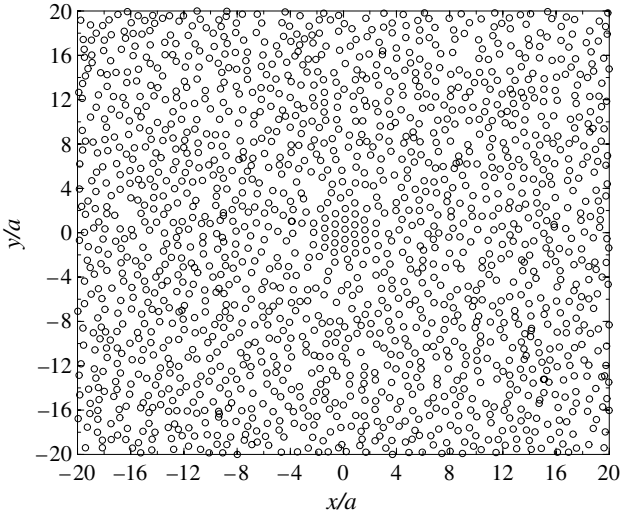

Figure 2. Simulation snapshot for parameters $\Gamma = 7.4$, $a_0 = 10$ and $\bar{l} = 2$. The colloidal particles are rendered as circles.

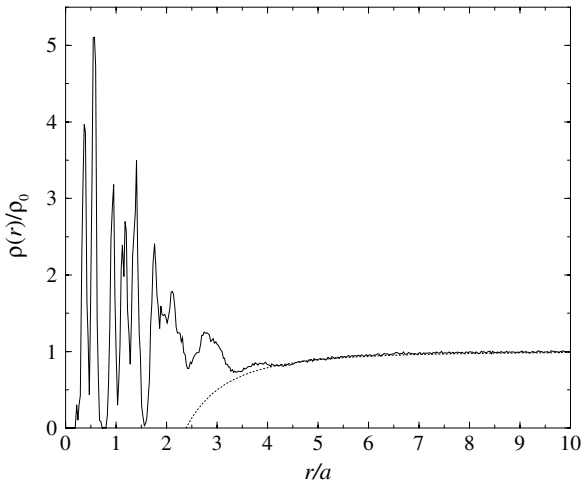

Figure 3. Inhomogeneous density profile (solid curve) for the parameters corresponding to figure 2. The asymptotic behaviour of the profile is denoted by the dotted curve, which represents the function $\rho(r)/\rho_0 = -13.5/(r/a)^3 + 1$.

particles interacting via a repulsive potential $\beta v(x) = \Gamma/(2x^3)$ in two dimensions takes place at $\Gamma_c = 135.5$ [19]. In figure 2 we show a simulation snapshot for a trap with strength $a_0 = 10$ and width $\bar{l} = 2$. It can be seen that the strong magnetic field in the middle attracts particles locally, which form a crystalline ordering. The latter is also witnessed by the sharp peaks in the inhomogeneous density $\rho(r)$ shown in figure 3. The highly concentrated region in the middle of the trap, which is also strongly localized because of the rather narrow width of the latter, creates a strong repulsion to the rest of the system that results into a local 'depletion zone' of magnetic colloids around the trap. This region can be discerned as an 'empty ring' in figure 2

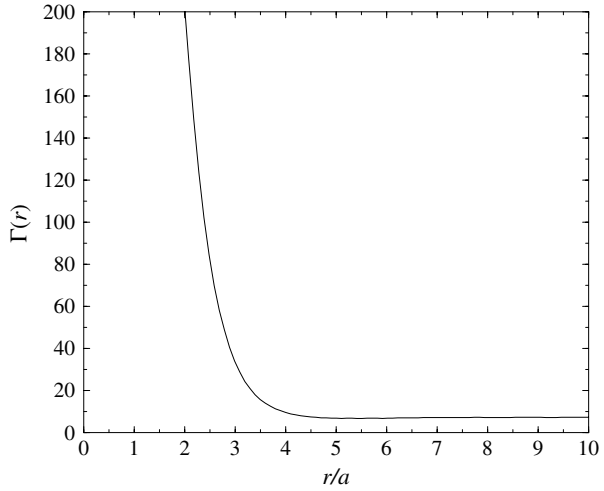

Figure 4. The averaged local coupling constant $\Gamma(r)$ for the parameters corresponding to figure 2.

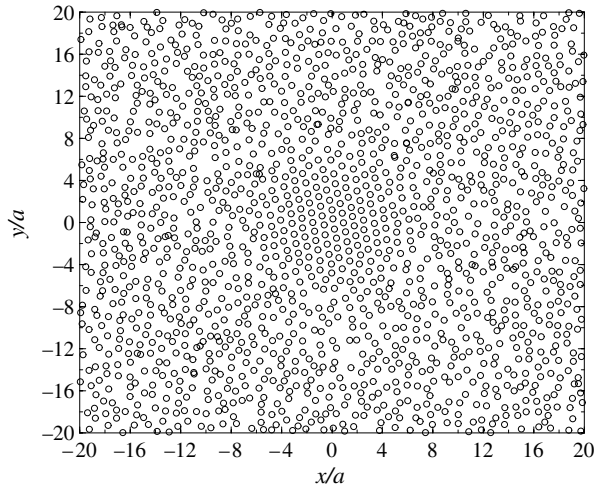

Figure 5. Simulation snapshot for parameters $\Gamma = 7.4$, $a_0 = 10$ and $\bar{l} = 4$.

and also as a depression of the density profile in figure 3 in the region $3 \lesssim r/a \lesssim 4$. Although there is an accumulation of particles in the middle of the trap, the depletion ring causes an overall *negative* coverage, $C = -9.3$ in this case. According to general arguments put forward by de Gennes [20], the inhomogeneity of the system in the middle acts as an external potential to the rest of it, and thus causes an asymptotic behaviour of the density profile of the form

$$\rho(r) - \rho_0 \sim 1/r^3, \qquad r \to \infty. \tag{13}$$

The dotted curve in figure 3 is precisely a fit of the form (13) above, $\rho(r)/\rho_0 - 1 = -13.5/(r/a)^3$.

The crystalline order in the centre of the trap is due to the high value of the magnetic field there which translates itself into a correspondingly high local value of the coupling constant

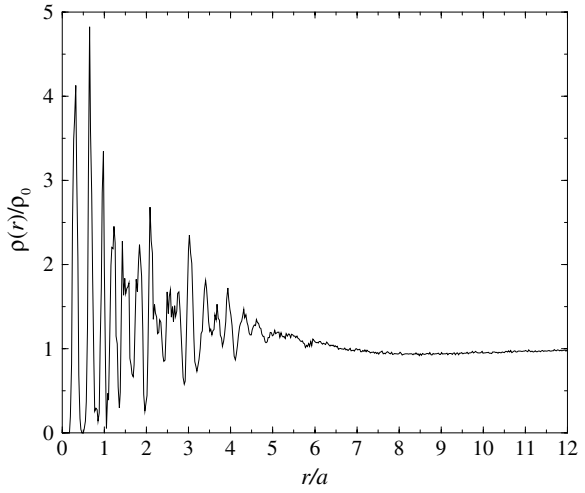

Figure 6. The density profile for the parameters corresponding to figure 5.

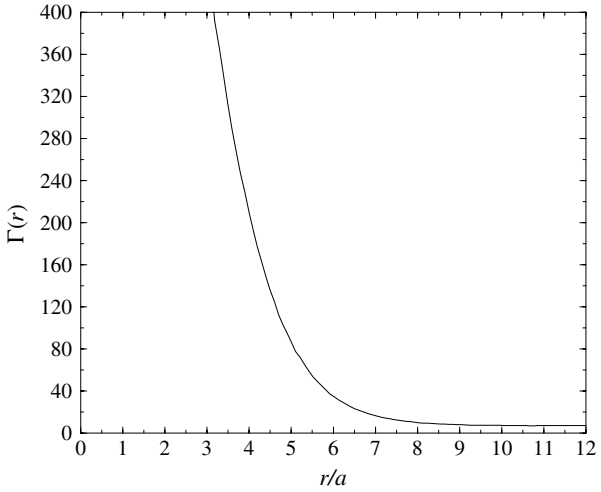

Figure 7. The averaged local coupling constant $\Gamma(r)$ for the parameters corresponding to figure 5.

Γ. In order to define this quantity in a physically meaningful way, we first construct a locally averaged *weighted density* $\bar{\rho}(r)$ as follows [21]:

$$\bar{\rho}(r) = \frac{1}{\pi\sigma^2} \int \Theta(\sigma - |\mathbf{r} - \mathbf{r}'|)\rho(r')\,\mathrm{d}^2 r', \tag{14}$$

where $\Theta(z)$ is the Heaviside step-function and σ is a length scale that limits the region within which the local averaging is carried out. There is some arbitrariness in the choice of σ; however, this quantity should be neither smaller than a, so that the local interactions can be taken into account, nor much larger than it, since in that case the local character of the coupling would be lost. We therefore choose $\sigma = 2a$ and define with the help of $\bar{\rho}(r)$ the local coupling constant $\Gamma(r)$, in analogy to equation (7), as

$$\Gamma(r) = \frac{(\chi B_0(r))^2}{k_\mathrm{B}T} \left(\pi\overline{\rho}(r)\right)^{3/2}. \tag{15}$$

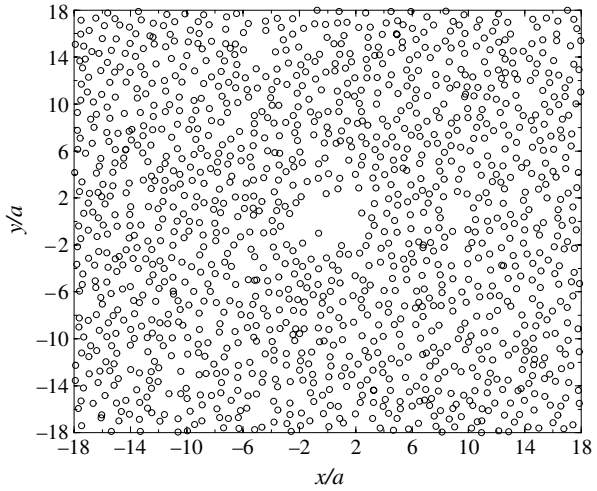

Figure 8. Simulation snapshot for the parameter combination $\Gamma = 5.7$, $a_0 = -1.5$ and $\bar{l} = 1.9$.

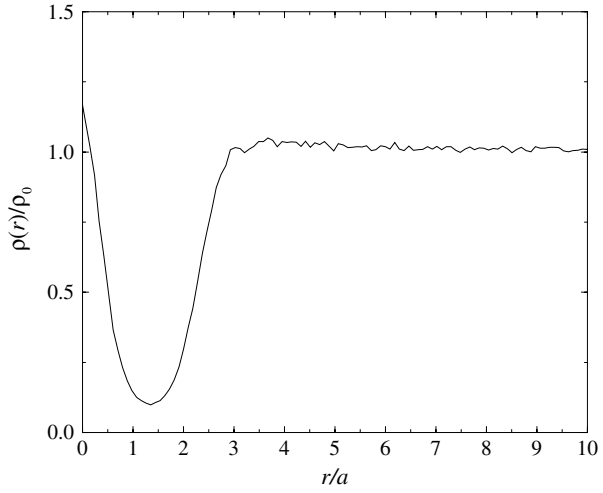

Figure 9. The density profile for the parameters corresponding to figure 8.

The local coupling constant is plotted in figure 4. The domain of crystallinity, $r/a \lesssim 2.5$, coincides with the region in which $\Gamma(r)$ exceeds the critical freezing value, $\Gamma_c = 135.5$, mentioned above.

The effect of increasing the width of the trap is shown in figure 5, pertaining to $\Gamma = 7.4$ and $a_0 = 10$, as before, but now $\bar{l} = 4$. Once again, a crystalline domain appears in the trap region, whose domain is extended in comparison to the case of the narrow trap examined before. As a result of the smoother decay of the inhomogeneous field towards its asymptotic value, the interface between the crystalline and the fluid phase is less sharp. In particular, the local depletion region visible in figure 2 is absent in this case, since the local lattice constant is changing smoothly from its value in the crystal phase to the corresponding one in the fluid phase. As seen in figure 6, the depletion zone is now longer-range but much shallower than before. The net effect on the coverage C turns out to be positive in this case, and the number

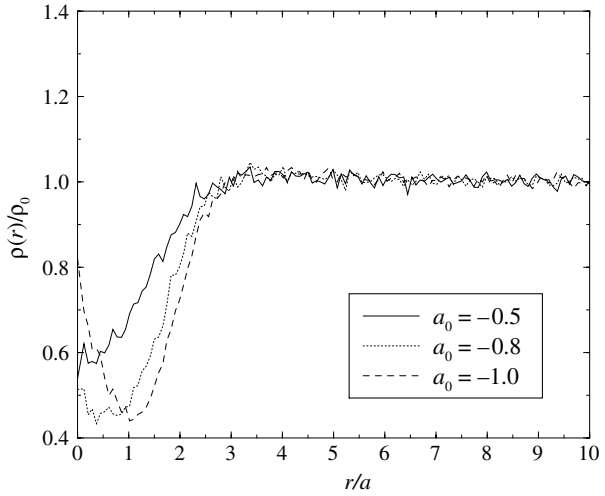

Figure 10. Inhomogeneous density profiles for the parameter combination $\Gamma = 7.4$, $\bar{l} = 2$ and several different values $a_0 < 0$, as indicated in the legend. The corresponding coverages are given in the text.

$C = 12.1$ is obtained. Thus, for the case $a_0 > 0$, the coverage coefficient C has a non-monotonic dependence on the trap parameters and can change sign, depending on the width of the inhomogeneous external field. In the latter case there is particle trapping. The local coupling constant $\Gamma(r)$ is shown in figure 7; once more, the region of crystallinity roughly coincides with the region $\Gamma(r) > \Gamma_c$.

There are two extreme cases of inhomogeneous profiles. One is a δ-function peak, where a single particle is trapped in the middle, repelling all the other particles. In this case the depletion zone is very deep, and coverage C is negative. The opposite of a δ-peak is a very slowly varying inhomogeneous profile with $\bar{l} \gg 1$. Then the depletion zone is very shallow and the coverage is positive. Therefore, changing the width of the Gaussian trap allows direct control of the coverage C.

We now turn our attention to the opposite case, $a_0 < 0$, in which the superimposed inhomogeneous field points in a direction opposite to $\mathbf{B}_0$. In this way, a local depression of the total magnetic field is created at the centre, and the field–particle interaction increases. A void in the local density results, as can be seen in figure 8, which pertains to parameters $\Gamma = 5.7$, $a_0 = -1.5$ and $\bar{l} = 1.9$. The corresponding density profile is shown in figure 9, and the resulting coverage is in this case negative, $C = -12.2$. The density peak in the centre of the inhomogeneous field is due to the fact that $|a_0| > 1$. Thus, the amplitude $B_0(r)$ of the total magnetic field displays a local maximum at the origin and, due to the third term in equation (4), there is a local particle accumulation there.

Tuning the strength of the external potential allows now for controlling externally the extent of the region that is depleted of colloidal particles. This is demonstrated in figure 10, in which density profiles for fixed values $\Gamma = 7.4$, $\bar{l} = 2$ and varying $a_0 < 0$ are shown. The corresponding coverages C are -6.0 for $a_0 = -1.0$, -5.4 for $a_0 = -0.8$, and -1.8 for $a_0 = -0.5$. Note that for the cases $a_0 = -0.5$ and $a_0 = -0.8$, for which $|a_0| < 1$, there is no local maximum at the origin, as the amplitude $B_0(r)$ of the total field has a global *minimum* there.

Of particular interest is the case in which $a_0 < -1$ and at the same time the width of the trap extends over a broad region, $\bar{l} \gg 1$. In this case, one obtains in the centre a local

field that points in a direction *opposite* to that of the field far away from the inhomogeneity. Correspondingly, the paramagnetic particles in the middle have opposite polarization than those far from it, hence they attract each other. One could create in this way a bulk-like crystalline region in the middle of the sample that *attracts* particles in the fluid-like region away from it, and a nontrivial interface is expected. We notice, however, that particles belonging to the two different regions still repel each other, since the sign of the magnetization of the colloidal particles flips as soon as the borderline $\mathbf{B}_0(\mathbf{r}) = 0$ is crossed. We will return to this problem in the future.

4. Conclusions

In conclusion, we have investigated how an inhomogeneous localized magnetic field acts on a suspension of magnetic particles in a uniform field. We have confirmed a magnetic tweezer effect for small densities, due to the attractive self-energy of an induced dipole in an external field. For higher densities many colloidal particle will be attracted by the trap, and this in turn induces a repulsive interparticle energy which competes against the attractive field–particle-energy, resulting in a depletion ring of particles around the trap. For larger colloidal densities close to freezing, the inhomogeneity will induce crystallites which are roughly extended across the inhomogeneity. The sign of the net coverage depends delicately on the range l of the inhomogeneity relative to the interparticle spacing. For a different sign of the inhomogeneous field relative to that of the homogeneous one, void formation (or 'hole burning') was observed. If the trapping field reverses the sign of the total field, particles are trapped again in the centre of the void.

Our effects can be verified in experiments using the typical set-up of two-dimensional magnetic colloids [11–14]. They can be exploited to control particle trapping or particle exclusion via the external field and should have an impact on possible applications of how to guide magnetic particle via fields, which is typically encountered for ferrofluids [22].

It would be interesting for future studies to predict our simulated density profiles by classical density functional theory of inhomogeneous fluids. Density functional theory can be straightforwardly applied to two spatial dimensions (for a recent work, see for example [23]), but a reliable approximation for soft interactions is still under debate.

Further future studies should focus on the inhomogeneous field caused by a single solenoid, which will necessarily have an in-plane component [24]. It is easier to realize this situation experimentally [25] since typically the microscope is placed on top of the sample. The in-plane component of the magnetic field will lead to a mutual attraction between the particle and can trigger chain formation around the inhomogeneity. All the set-ups studied in this paper are radially symmetric external fields. Another interesting inhomogeneity is a wedge-like field. Here one could speculate about true thermodynamic phase transitions such as a localization–delocalization transition as a function of the external field strength.

Acknowledgments

We thank Christoph Eisenmann and Georg Maret for helpful discussions. This work was supported by the DFG within the SFB TR6 (subproject C3).

References

[1] Ketterle W 2002 *Rev. Mod. Phys.* **74** 1131
[2] Resnick A 2003 *J. Colloid Interface Sci.* **262** 55
[3] Löwen H 2001 *J. Phys.: Condens. Matter* **13** R415
[4] Grier D G 2003 *Nature* **424** 810

[5] Meiners J C and Quake S R 1999 *Phys. Rev. Lett.* **82** 2211
[6] Bartlett P, Henderson S I and Mitchell S J 2001 *Phil. Trans. R. Soc.* A **359** 883
[7] Hoogenboom J P, Vossen D L J, Faivre-Moskalenko C, Dogterom M and van Blaaderen A C 2002 *Appl. Phys. Lett.* **80** 4828
[8] Bustamante C, Bryant Z and Smith S B 2003 *Nature* **421** 423
[9] Sullivan M, Zhao K, Harrison C, Austin R H, Megens M, Hollingsworth A, Russel W B, Cheng Z D, Mason T and Chaikin P M 2003 *J. Phys.: Condens. Matter* **15** S11
[10] Giordano N and Cheng J-T 2001 *J. Phys.: Condens. Matter* **13** R271
[11] Zahn K and Maret G 1999 *Curr. Opin. Colloid Interface Sci.* **4** 60
[12] Zahn K, Méndez-Alcaraz J M and Maret G 1997 *Phys. Rev. Lett.* **79** 175
[13] Zahn K, Lenke R and Maret G 1999 *Phys. Rev. Lett.* **82** 2721
[14] Zahn K and Maret G 2000 *Phys. Rev. Lett.* **85** 3656
[15] Wojciechowskii K and Klos J 1996 *J. Phys. A: Math. Gen.* **29** 3963
[16] Rothen F and Pieranski P 1996 *Phys. Rev.* E **53** 2828
[17] Froltsov V A, Blaak R, Likos C N and Löwen H 2003 *Phys. Rev.* E **68** 061406
[18] Frenkel D and Smit B 1996 *Understanding Molecular Simulation* (San Diego, CA: Academic)
[19] Löwen H 1996 *Phys. Rev.* E **53** R29
[20] de Gennes P G 1981 *J. Physique Lett.* **42** L377
See also the discussion about power-law tails for inhomogeneous Lennard-Jones fluids by Dietrich S 1988 *Phase Transitions and Critical Phenomena* vol 12, ed C Domb and J Lebowitz (London: Academic) p 1
[21] Evans R 1992 *Fundamentals of Inhomogeneous Liquids* ed D Hendenson (New York: Dekker)
[22] Odenbach S (ed) 2002 *Ferrofluids, Magnetically Controllable Fluids and Their Applications* (*Springer Lecture Notes in Physics* vol 594) (Berlin: Springer)
[23] Rasmussen L L and Oxtoby D W 2002 *J. Phys.: Condens. Matter* **14** 12021
[24] Jackson J D 1975 *Classical Electrodynamics* (New York: Wiley)
[25] Eisenmann C and Maret G 2004 private communication